Reorganization of Structural Connectivity in the Brain Supports Preservation of Cognitive Ability in Healthy Aging

Josh Neudorf[1,2], Kelly Shen[1,2], & Anthony R. McIntosh[1,2]

[1]Institute for Neuroscience and Neurotechnology, Simon Fraser University, Burnaby, Canada
[2]Department of Biomedical Physiology and Kinesiology, Faculty of Science, Simon Fraser University, Burnaby, Canada

* Corresponding author

E-mail: randy_mcintosh@sfu.ca (ARM)

Acknowledgements

This research was supported by the Natural Sciences and Engineering Research Council of Canada through Postdoctoral Fellowships Program funding to Josh Neudorf, and Discovery Grant *RGPIN-2018-04457* to the senior author Anthony R. McIntosh, and by Canadian Institutes of Health Research Project Grant *PJT-168980*. The authors affirm that there are no conflicts of interest to disclose.

Abstract

The global population is aging rapidly, and a research question of critical importance is why some older adults suffer tremendous cognitive decline while others are mostly spared. Past aging research has shown that older adults with spared cognition have better local short-range information processing while global long-range processing is less efficient. We took this research a step further to investigate whether the underlying structural connections, measured in vivo using diffusion magnetic resonance imaging (dMRI), show a similar shift to support cognitive ability. We analyzed the structural connectivity streamline counts and nodal efficiency and local efficiency regional graph theory metrics to determine if age and cognition are related to structural network differences. We found that the relationship between structural connectivity and cognition with age was nuanced, with some differences with age that were associated with poorer cognitive outcomes, but other reorganizations that were associated with spared cognitive ability. These changes included strengthened local intrahemispheric connectivity and increased nodal efficiency of the ventral occipital-temporal stream, nucleus accumbens, and hippocampus for older adults, and widespread local efficiency primarily for middle-aged individuals.

Keywords: structural connectivity, diffusion-weighted magnetic resonance imaging, graph theory, healthy aging, fluid intelligence

Reorganization of Structural Connectivity in the Brain Supports Preservation of Cognitive Ability in Healthy Aging

The global population is aging rapidly (Beard et al., 2016). We are at a crucial juncture for understanding and addressing cognitive decline in this population, as emphasized by the United Nations General Assembly's declaration that the decade from 2021 to 2030 is the Decade of Healthy Aging, calling for action to improve the health and well-being of the aging population (United Nations, 2022). Cognitive decline during aging is not an isolated concern, as it has also been shown to predict health outcomes years later (Nelson et al., 2020). This cognitive decline has been related to structural atrophy in the brain including cortical thinning (Salat et al., 2004) and myelin degradation (Bartzokis, 2004). However, research has also identified functional changes in how older adults process information that has been explained as a functional adaptation to the negative structural changes occurring (Cabeza et al., 2002; Davis et al., 2008).

Although changes in brain structural and functional connectivity have been associated with brain aging (Coelho et al., 2021; Damoiseaux, 2017; Pur et al., 2022), a demonstration that aspects of the structural connectivity network may *support* cognition in older age represents an important gap in the current literature. There is, in many cases, an implicit assumption that changes with age impact an individual negatively, but by including cognitive measures in addition to age in our models we can investigate whether there are connectivity changes that impact cognitive ability positively. This idea has been supported by electroencephalography (EEG) functional research showing that local complexity (involved in short-range, intrahemispheric interactions) increases with older age, while global complexity (involved in longer range, interhemispheric interactions) decreases. Interestingly, this pattern was associated with better cognition in older adults (Heisz et al., 2015). This supports the notion that not all brain changes in older age are negative, but rather that there may be mechanisms that help the brain to retain cognitive ability in the face of other physiological brain changes.

Functional connectivity represents a valuable measure of how regions work in tandem in the brain, while structural connectivity represents the physical, observable connections that evolve over the lifespan. This structural connectivity network in the brain ultimately constrains the functional states that the brain can occupy (Gu et al., 2015), and continuing research has led to growing estimates of the extent to which functional activity and functional connectivity can be accounted for based on the underlying structural connectivity (Ekstrand et al., 2020; Goñi et al., 2014; Hagmann et al., 2008; Honey et al., 2010; Neudorf et al., 2020, 2022; Rosenthal et al., 2018; Sarwar et al., 2021; Schirner et al., 2018). Knowing where there are physical changes in the brain network with age could allow for valuable interventions and prevention strategies for older adults. The whole-brain network effects of these changes are vast, varied, and challenging to assess, but graph theory approaches (Sporns, 2018) have allowed the network neuroscience research community to make great strides towards understanding the brain when viewed as a network.

In the current paper, we will investigate the relationship between structural connectivity in the aging brain and cognitive measures from a number of analytic and graph theory perspectives. The link between connectivity and cognition in older age has been investigated using whole-brain graph theory measures of structural and functional connectivity, but structural connectivity was not associated with changes in fluid intelligence (Madden et al., 2020). In many cases, research has focused on single whole-brain measures of connectivity rather than studying the heterogeneous changes that may occur in different regions. We address the limitations of the single whole-brain measure approach by investigating the connection-specific changes and regional graph theory measures to understand the characteristics throughout the network that hinder and/or support cognition in older age. We will investigate how structural connectivity streamline counts are associated with cognition and age, before investigating this relationship using regional graph theory measures of nodal and local efficiency. We hypothesize that this relationship will be nuanced as it is for functional analyses (Heisz et al., 2015), including some changes that are detrimental to cognition, but also changes that help to spare cognition in older age.

Methods

Data came from the Cambridge Centre for Ageing and Neuroscience (Cam-CAN; Shafto et al., 2014) dataset. This data was collected in compliance with the Helsinki Declaration, and was approved by the local ethics committee, Cambridgeshire 2 Research Ethics Committee (reference: 10/H0308/50). The structural connectivity (SC) measures of streamline count and distance were calculated from the diffusion-weighted magnetic resonance imaging (dMRI) data using the TheVirtualBrain-UK Biobank pipeline (Frazier-Logue et al., 2022), which uses probabilistic tractography (*FSL probtrackx*; Hernandez-Fernandez et al., 2019; Jenkinson et al., 2012). These SC streamline counts were calculated between all combinations of the 218 regions of interest in a combined atlas of the Schaefer 200 region atlas (Schaefer et al., 2018) and the subcortical Tian atlas (Tian et al., 2020). The subcortical regions were comprised of regions from the Tian Scale 1 atlas excluding the hippocampus. For hippocampus, the Scale 3 atlas was used with the two head divisions collapsed into a single parcel. The globus pallidus was excluded due to a large number of erroneous connections to/from this region, resulting in a total of 18 subcortical regions. The SC matrices were consistency thresholded (at least 50% of participants have the connection) and participants' data were excluded if they did not have behavioural data, had regions with no connections, or had SC density (number of non-zero connections divided by the total number of possible connections) 3 standard deviations (SD) or more away from the mean (retained N = 594 from the total of 656 participants in the dataset). The Cattell Culture Fair fluid intelligence score (Cattell & Cattell, 1973) was used to measure cognitive function. This measure of cognitive ability declines significantly with age in this population, $R(592) = -.651$, $p < .001$ (see Figure 1), so factors that counteract this decline represent a sparing of cognitive ability.

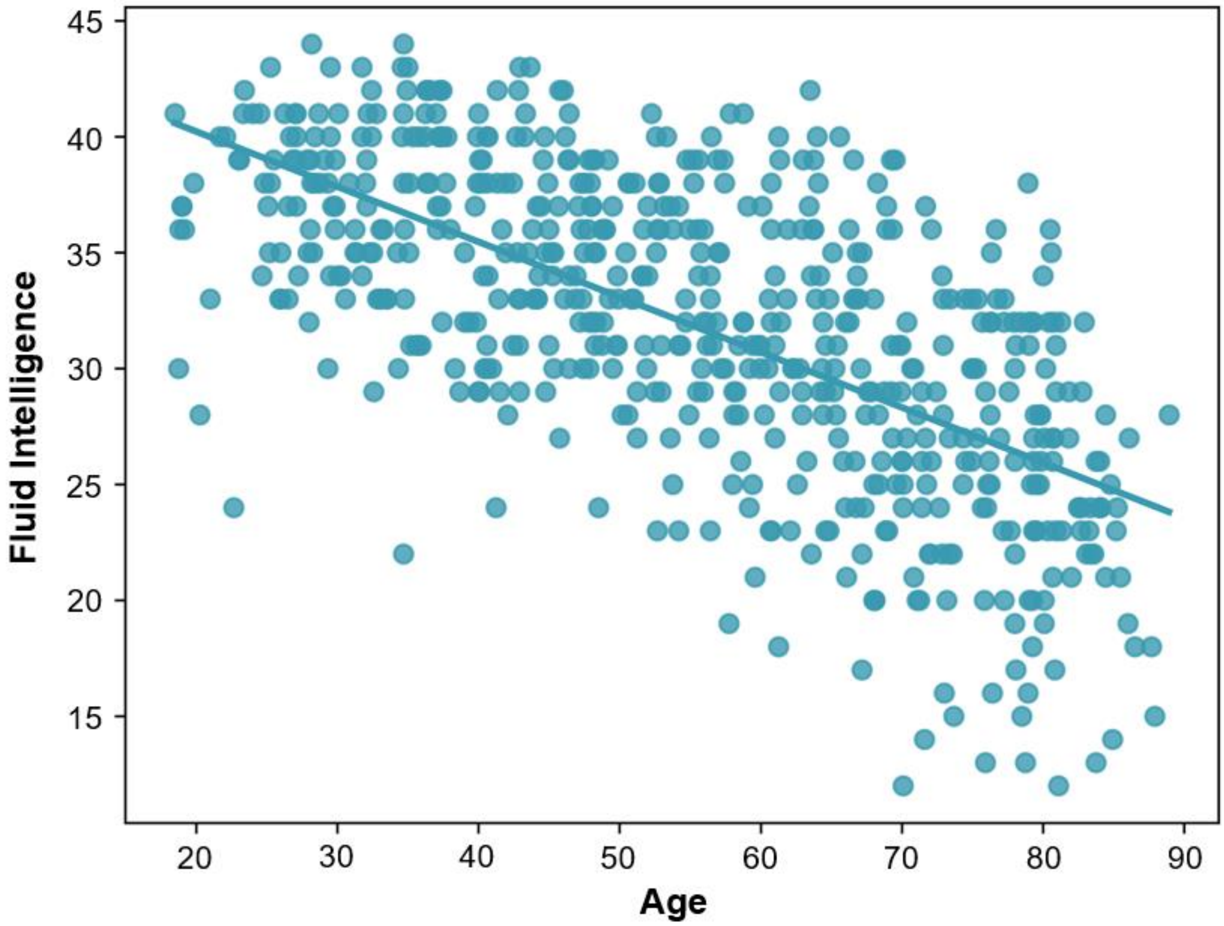

Figure 1. Relationship between age and fluid intelligence as measured by the Cattell Culture Fair fluid intelligence score. Fluid intelligence decreases significantly with age, $R(592) = -.651$, $p < .001$.

Participant ages ranged from 18.50 to 88.92 (mean = 55.414, *SD* = 18.090). Younger adults (YA; age < 50) ranged from 18.50 to 49.92 (mean = 36.966, *SD* = 8.385, *N* = 244) and older adults (OA; age > 50) ranged from 50.17 to 88.92 (mean = 68.275, *SD* = 10.163, *N* = 350).

Multivariate partial least squares (PLS) analysis (McIntosh & Lobaugh, 2004) was used to identify latent variables (LVs), each containing weights that describe the relationship of all connections with behaviour. We report only the most reliable PLS weights as determined by bootstrap resampling (bootstrap ratios; BSR). PLS (Kovacevic et al., 2013; McIntosh & Lobaugh, 2004) was performed using 1000 iterations for bootstrap sampling and permutation testing. Age and fluid intelligence were examined as dependent variables, with three separate PLS analyses for SC streamline count, as well as graph theory measures of SC-based nodal efficiency (NE), and SC-based local efficiency (LE). Nodal efficiency is a measure that is high for hub regions in the brain (van den Heuvel & Sporns, 2013), and is calculated as the mean of the inverse shortest path length to all other regions in the network,

$$E_{nodal}(j) = \frac{1}{N-1}\sum_{i}\frac{1}{l_{ij}}, \qquad (1)$$

where l_{ij} is the weighted shortest path length between regions i and j. Local efficiency is a separate measure of efficiency distinct from nodal efficiency, which is calculated as the mean of the inverse shortest path length for the subnetwork of connected regions after first removing the region of interest,

$$E_{local}(i) = \frac{1}{N_{G_i}(N_{G_i}-1)}\sum_{j,h\in G_i}\frac{1}{l_{jh}}, \qquad (2)$$

where G_i is the subgraph/subnetwork made up of the neighboring regions connected to region i, N_{G_i} is the number of regions in this subgraph, and l_{jh} is the weighted shortest path length between regions j and h in this subgraph. Local efficiency is thus a measure of how well connected the neighbors of a region are, and can been conceptualized as a measure of fault tolerance, or robustness against disruption to the network (Fornito et al., 2016).

Once significant regions were identified based on these graph theory measures, a supplementary rolling correlation analyses was conducted to identify critical periods during which these graph theory measures were most highly related to cognitive ability. This type of analysis is implemented in many statistical packages, and has been used in the analysis of financial time-series data (e.g., Ilalan & Pirgaip, 2019). The rolling correlation analysis consisted of selecting bins of participants with a range of 10 years of age and calculating the Pearson's R correlation coefficient between the mean graph theory measure and the fluid intelligence score. Bins of this size resulted in a mean number of participants in each bin of 91.532, with a standard deviation of 14.330, ranging from 42 to 111. Of the 62 total bins, 54 (87%) had over 80 participants, and bins with fewer participants were largely situated in the 7 youngest age bins. The confidence intervals of these correlation coefficients was calculated using the bias-corrected and accelerated bootstrap method (Efron, 1987), in order to determine whether the confidence intervals did not show extreme fluctuations across age bins.

Results

SC Streamline Count PLS

The PLS analysis of SC streamline count identified 2 significant LVs. LV1 (permutation $p < .001$) was negatively correlated with age, $R = -.813$, *95% CI* = [-.852, -.811], and positively correlated with fluid intelligence, $R = .615$, *95% CI* = [.613, .682], indicating that more streamlines in positively weighted connections related to better cognition in younger age. On the other hand, negative connection weights indicate that fewer streamlines in these connections related to better cognition in younger age. LV2 (permutation $p = .045$) was positively correlated with both age, $R = .313$, *95% CI* = [.067, .371] and fluid intelligence, $R = .300$, *95% CI* = [.283, .512], indicating that more streamlines with positive weights related to better cognition in older age. Negative weights, meanwhile, indicate that fewer streamlines in these connections related to better cognition in older age.

Latent Variable 1: Positive Weights

The largest positive weights from LV1 identified a subnetwork with roughly equal numbers of intrahemispheric (41.7%; 13.9% LH and 27.8% RH) and interhemispheric (58.3%) connections. Notable regions with a degree (number of connections) of at least 3 included bilateral medial parietal cortex, bilateral postcentral gyrus, LH dorsal prefrontal cortex (dPFC), LH precuneus, RH medial prefrontal cortex (mPFC), and RH hippocampus tail (see Figure 2). Of these regions, the two superior frontal regions, hippocampus, and precuneus have been previously identified as rich-club regions in the brain (highly connected hub regions that are also highly connected to one another; van den Heuvel & Sporns, 2011).

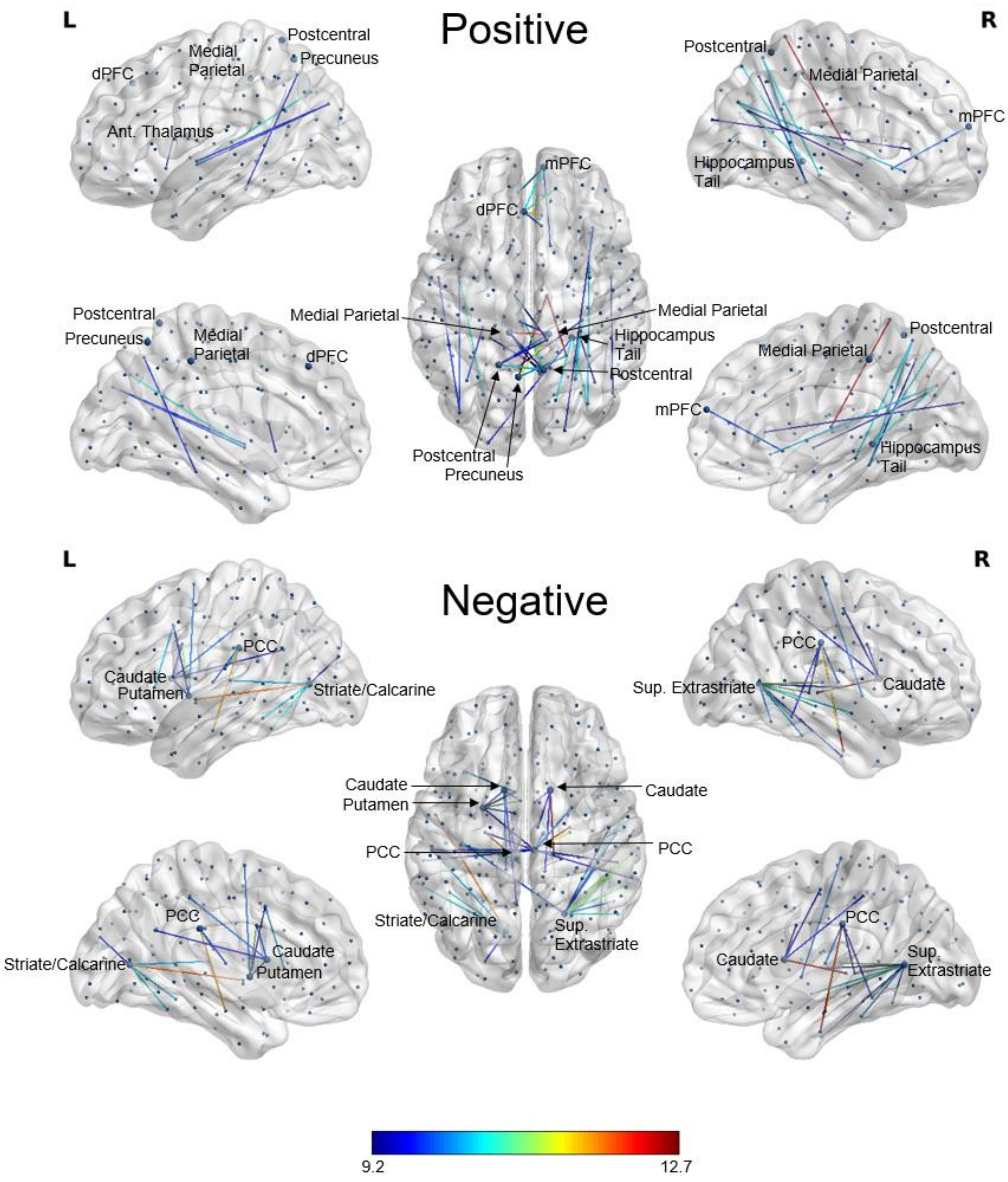

Figure 2. SC PLS analysis of age and cognition. Shown are LV1's most important connections as identified by bootstrap resampling. Connection color corresponds to the value of the bootstrap ratio (BSR) for that connection. The BSR threshold was selected to keep the number of displayed connections comparable for LV1 and LV2. Highly connected regions with degree (number of connections) greater than 3 are labeled.

Latent Variable 1: Negative Weights

The largest negative weights from LV1 identified a subnetwork made up of mostly intrahemispheric connections (87.8%; 39.0% LH and 48.8% RH), with the exception of 5 (12.2%) interhemispheric connections (1 to the RH superior extrastriate and 4 to the RH posterior cingulate cortex; PCC). Highly implicated regions in this network include the bilateral PCC, bilateral caudate nucleus, LH striate/calcarine cortex, LH putamen, and RH superior extrastriate (see Figure 2). In combination, LH striate/calcarine and RH superior extrastriate play a role in approximately half of the connections (48.8%).

Latent Variable 2: Positive Weights

For LV2, the largest positive weights were primarily intrahemispheric (94.1%) and split equally between the LH (47.1%) and RH (47.1%), with a small number of interhemispheric connections identified (5.9%; see Figure 3).

Latent Variable 2: Negative Weights

The largest negative weights for LV2 included mostly intrahemispheric connections (76.9%; 61.5% LH and 15.4% RH) with a smaller number of interhemispheric connections (23.1%). Highly implicated regions include the bilateral insula, LH frontal operculum, LH central sulcus, LH precuneus, RH anterior thalamus, and RH hippocampus tail(see Figure 3).

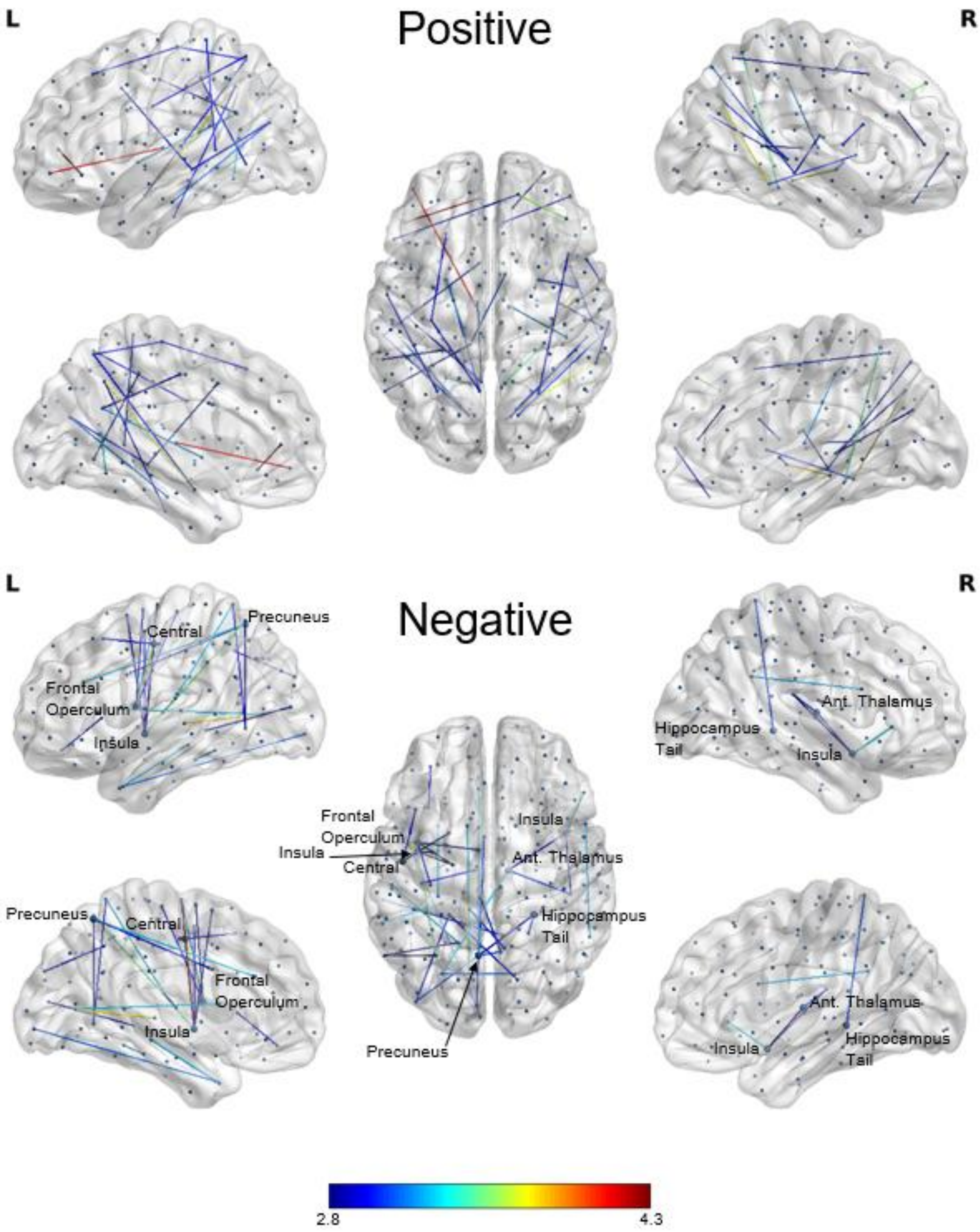

Figure 3. SC PLS analysis of age and cognition. Shown are LV2's most important connections as identified by bootstrap resampling. Connection color corresponds to the value of the bootstrap ratio (BSR) for that connection. The BSR threshold was selected to keep the number of displayed connections comparable for LV1 and LV2. Highly connected regions with degree (number of connections) greater than 3 are labeled.

SC Nodal Efficiency PLS

Younger Adults

The SC nodal efficiency PLS analysis for YAs identified 1 significant LV. This LV (permutation $p = .012$) was negatively correlated with age, $R = -.482$, *95% CI* = [-.616, -.459], and positively correlated with fluid intelligence, $R = .113$, *95% CI* = [.047, .266], indicating that higher nodal efficiency in positively weighted regions related to better cognition in younger age. On the other hand, negative region weights indicate that lower nodal efficiency in these regions contribute to better cognition in younger age.

For these YA, PLS identified a striking pattern of negative connection weights in the insula and lateral prefrontal cortex, indicating that less nodal efficiency is better for cognition in these regions. These regions include bilateral insula, bilateral ventrolateral and dorsolateral prefrontal cortex, and bilateral putamen. There were also positively weighted regions indicating that more nodal efficiency is better for cognition in these regions. These regions included the LH precuneus, LH striate, LH mPFC, LH hippocampus, RH striate and extrastriate, RH inferior parietal lobule, and RH temporal pole (see Figure 4).

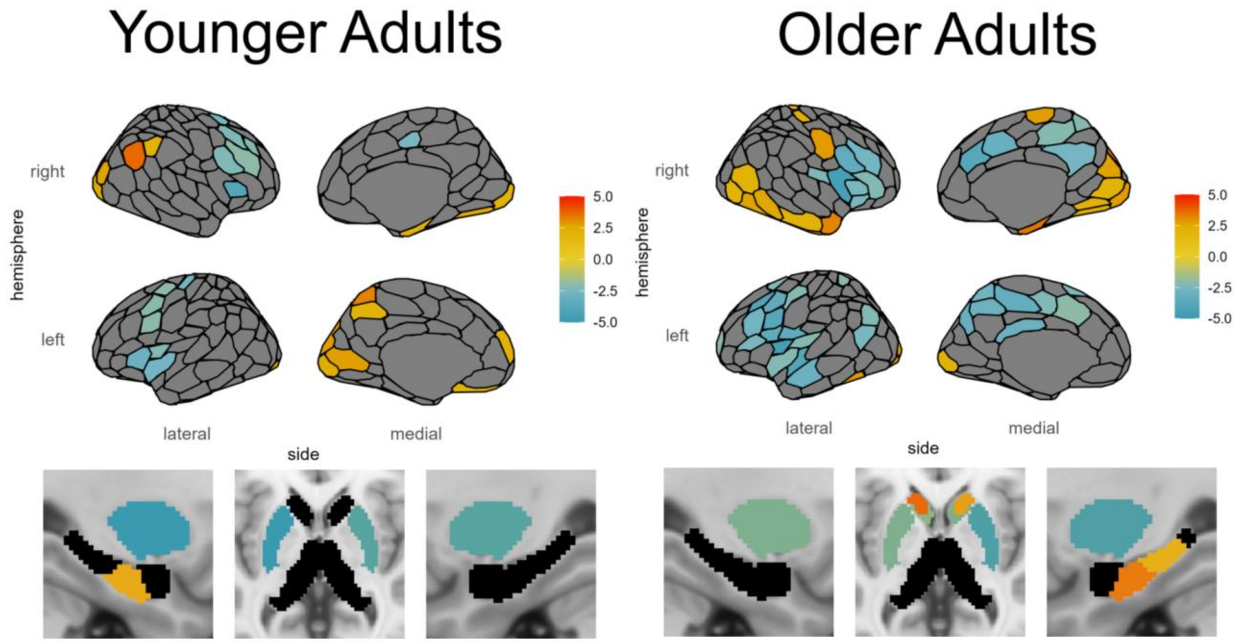

Figure 4. SC-based nodal efficiency PLS analysis of age and cognition. Shown are the connections identified as significant with respect to the correlation with age and cognition. Region color corresponds to the value of the bootstrap ratio (BSR) for that region, thresholded at ±2.0.

Older Adults

The PLS analysis for OAs identified 1 significant LV. This LV (permutation $p < .001$) was negatively correlated with age, $R = -.467$, *95% CI* = [-.632, -.428], and positively correlated with fluid intelligence, $R = .316$, *95% CI* = [.289, .482], indicating that higher nodal efficiency in positively weighted regions related to better cognition in younger age. On the other hand, negative region weights indicate that lower nodal efficiency in these regions contributed to better cognition in younger age.

For these OA, PLS identified a similar striking pattern of negative connection weights as was seen in the YA, but with more regions involved bilaterally in medial parietal regions, medial and lateral frontal regions, and the caudate nucleus, and greater involvement in the LH superior temporal lobe and LH auditory cortex. For the positively weighted regions indicating better cognition, PLS identified a greater number of regions than the YA, including bilateral nucleus accumbens and a striking pattern of regions in the RH, including the striate, extrastriate, and ventral occipital-temporal stream, with involvement of this ventral stream all the way to the temporal pole, as well as postcentral gyrus and hippocampus (see Figure 4).

Rolling Correlation Analysis: Nodal Efficiency and Cognition

In order to investigate whether there may have been a critical age period during which nodal efficiency was beneficial for cognition in the regions identified as being positively related to cognition in OA, a rolling Pearson's R correlation coefficient analysis between the mean nodal efficiency in these regions and cognition was calculated with a window size of 10 years (see Figure 5). The size of confidence intervals appeared consistent across the different age bins. This analysis revealed an inverted 'U' shape in this relationship, and identified a critical period during which the nodal efficiency of these regions was beneficial for cognition, during the ages of approximately 55-72 years.

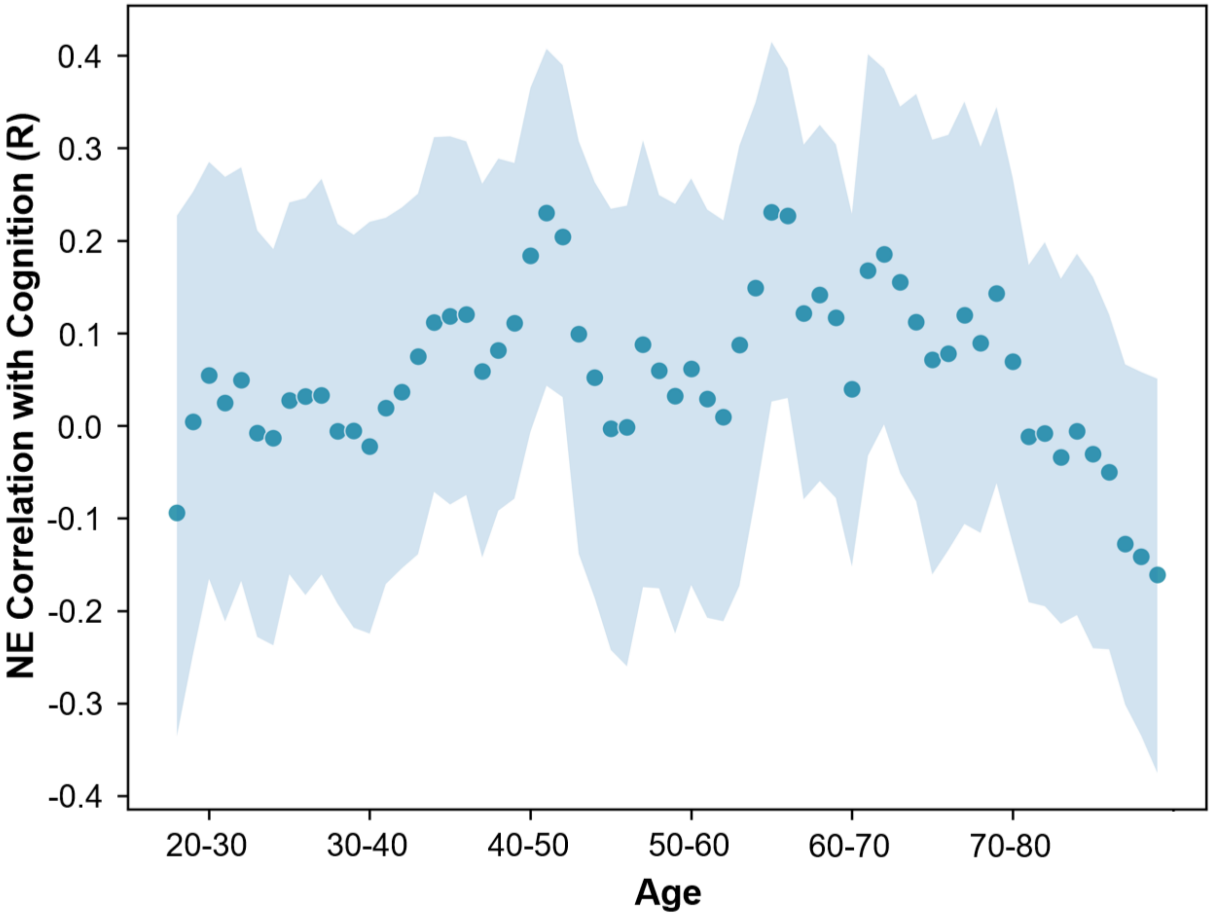

Figure 5. Rolling Pearson's R correlation coefficient between mean nodal efficiency for regions positively related to the PLS LV in OA and cognition for participants in age windows of 10 years. Shaded area represents the 95% CI.

Mean Nodal Efficiency

To better understand the pattern of negatively weighted regions with respect to nodal efficiency, we also present the mean nodal efficiency values (see Figure 6). The pattern of higher nodal efficiency hub-like regions overlapped with those regions identified as being negatively related to cognition, especially for OA but also for YA, particularly in the insula, lateral PFC, cingulate cortex, medial parietal regions, putamen, and caudate nucleus. This overlap suggests that there may be an optimal network configuration of hub regions in the brain, and that alterations to this configuration were detrimental to cognition.

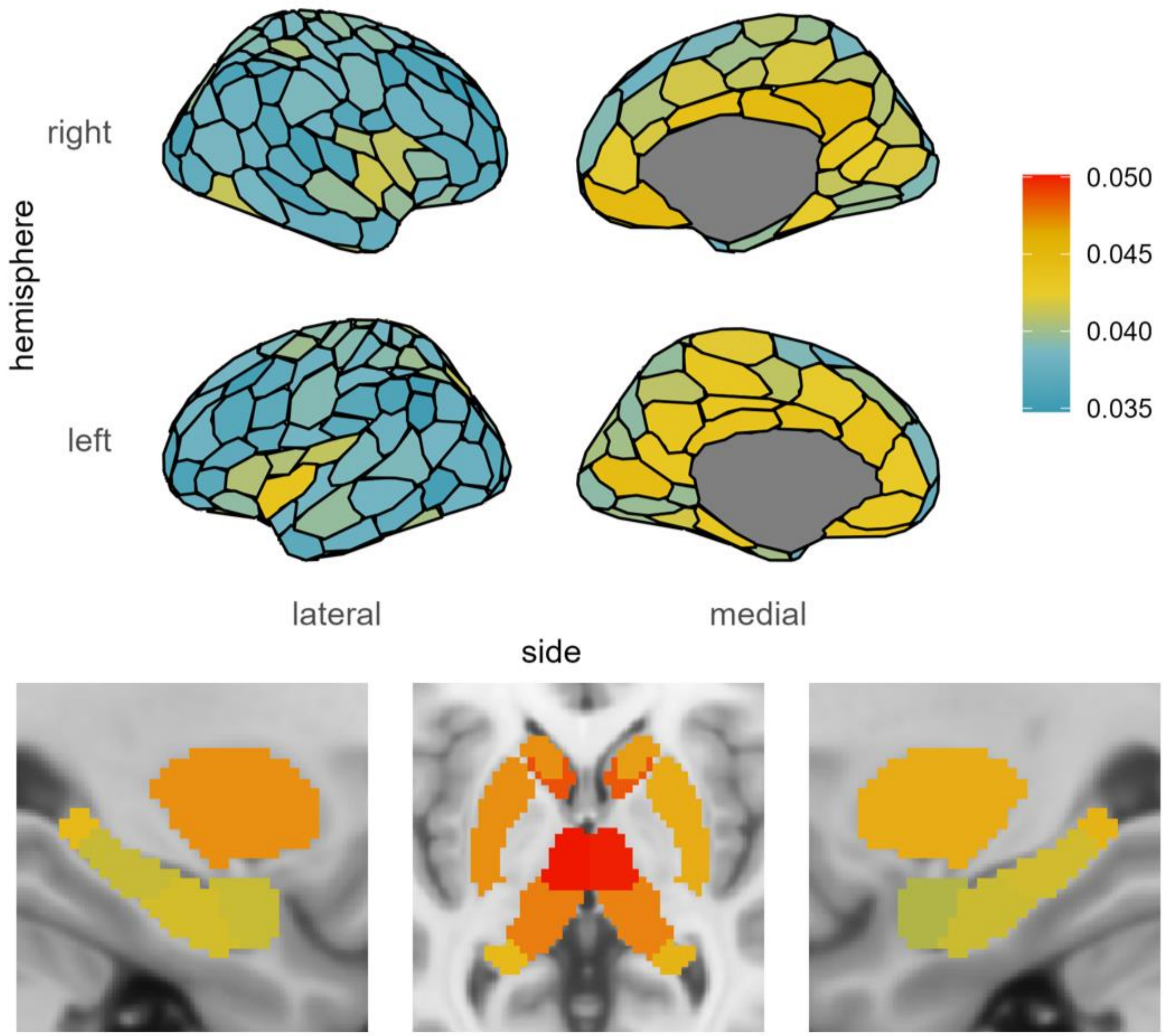

Figure 6. Brain map of mean nodal efficiency for all participants.

SC Local Efficiency PLS

Younger Adults

The SC local efficiency PLS analysis for YAs identified 1 significant LV. This LV (permutation $p < .001$) was negatively correlated with age ($R = -.352$, *95% CI* = [-.548, -.309]) and positively correlated with fluid intelligence ($R = .134$, *95% CI* = [.081, .263]), indicating that higher local efficiency in positively weighted regions related to better cognition in younger age.

On the other hand, negative region weights indicate that lower local efficiency in these regions contributed to better cognition in younger age.

For these YA, local efficiency was positively related to cognition in the large majority of regions, including bilateral cingulate cortex, bilateral precuneus, bilateral retrosplenial cortex, bilateral medial parietal cortex, bilateral temporal and temporoparietal cortex, bilateral auditory cortex, LH hippocampus body, RH parahippocampal cortex, RH superior and inferior extrastriate, RH postcentral gyrus, RH precentral gyrus, RH dorsal prefrontal cortex, RH insula, RH posterior thalamus, and RH hippocampus, with a smaller number of negatively related regions in the bilateral orbitofrontal cortex, bilateral ventral prefrontal cortex, bilateral anterior thalamus, LH central sulcus, and LH inferior parietal sulcus (see Figure 7).

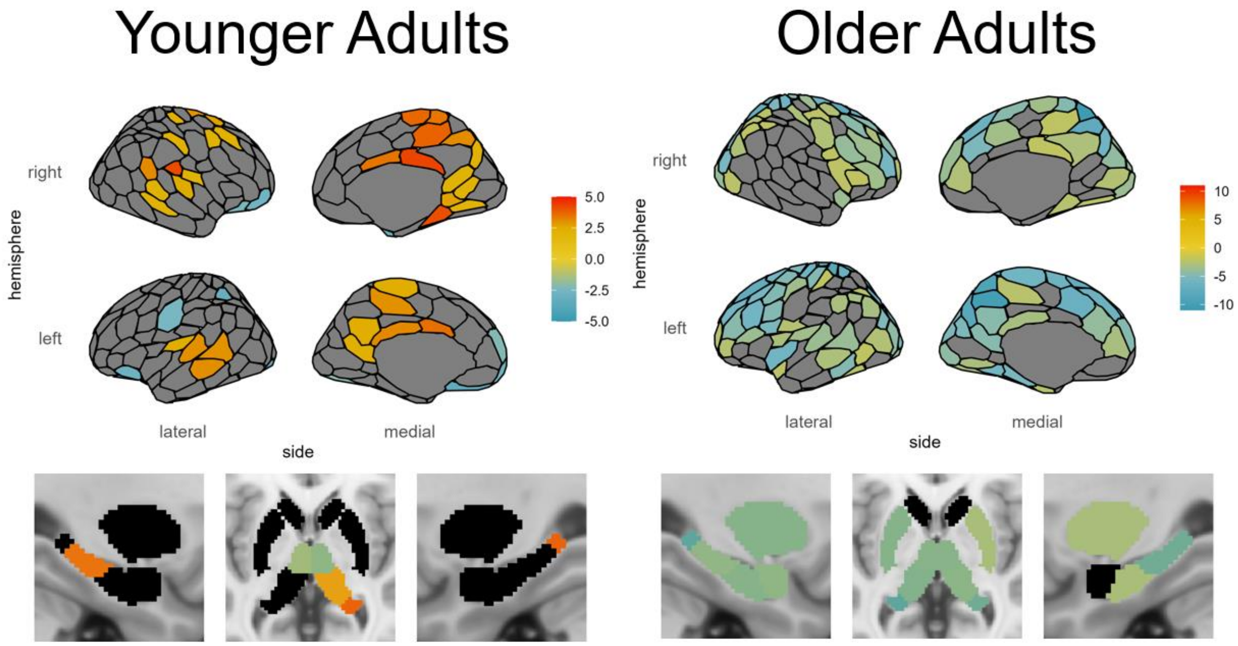

Figure 7. SC-based local efficiency PLS analysis of age and cognition. Shown are the connections identified as significant with respect to the correlation with age and cognition. Region color corresponds to the value of the bootstrap ratio (BSR) for that region, thresholded at ± 2.0.

Older Adults

The PLS analysis for OAs identified 1 significant LV. This LV (permutation $p < .001$) was negatively correlated with age, $R = -.430$, *95% CI* = [-.576, -.354], and positively correlated with fluid intelligence, $R = .274$, *95% CI* = [.230, .405], indicating that higher local efficiency in positively weighted regions related to better cognition in younger age. On the other hand, negative region weights indicate that lower local efficiency in these regions contributed to better cognition in younger age.

Unlike the YA, for these OA local efficiency was negatively related to cognition in all significant regions, which were distributed throughout large portions of the brain (see Figure 7).

Rolling Correlation Analysis: Local Efficiency and Cognition

To investigate whether there may be a critical age period during which local efficiency is beneficial for cognition in the regions identified as being positively related to cognition in YA, a rolling Pearson's R correlation coefficient analysis between the mean nodal efficiency in these regions and cognition was calculated with a window size of 10 years (see Figure 8). The sizes of confidence intervals appeared consistent across the different age bins. This analysis revealed a critical period during which the nodal efficiency of these regions was beneficial for cognition, during the ages of approximately 32-51 years.

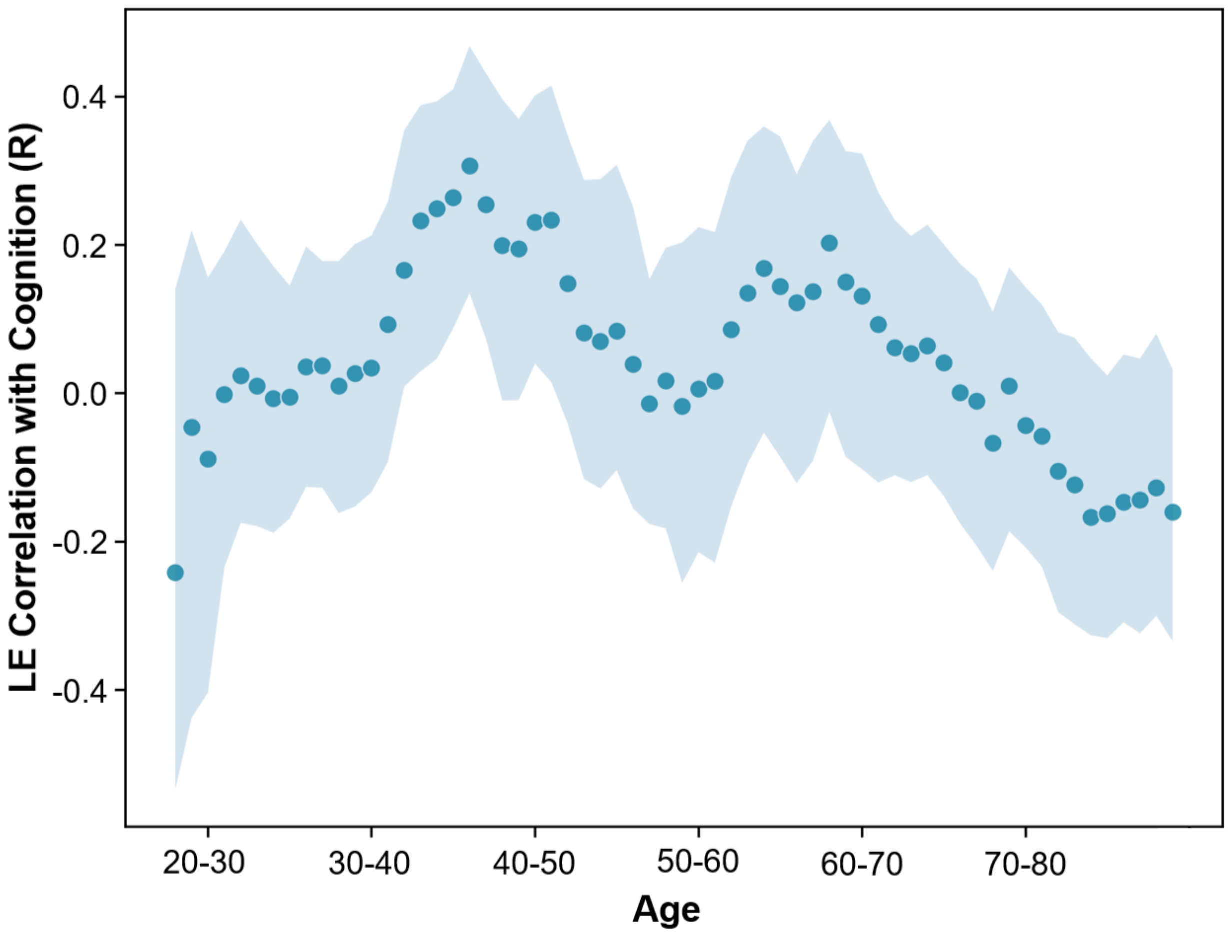

Figure 8. Rolling Pearson's R correlation coefficient between mean local efficiency for regions positively related to the PLS LV in YA and cognition for participants in age windows of 10 years. Shaded area represents the 95% CI.

Whole-brain Network Effects of Local Efficiency

Mean local efficiency (in the regions identified as negatively associated with cognition in OA; see Fig. 7) had no significant relationship with age in YA, $R(242) = -.094$, $p = .143$, but a strong positive relationship with age in OA, $R(348) = .461$, $p < .001$ (see Figure 9).

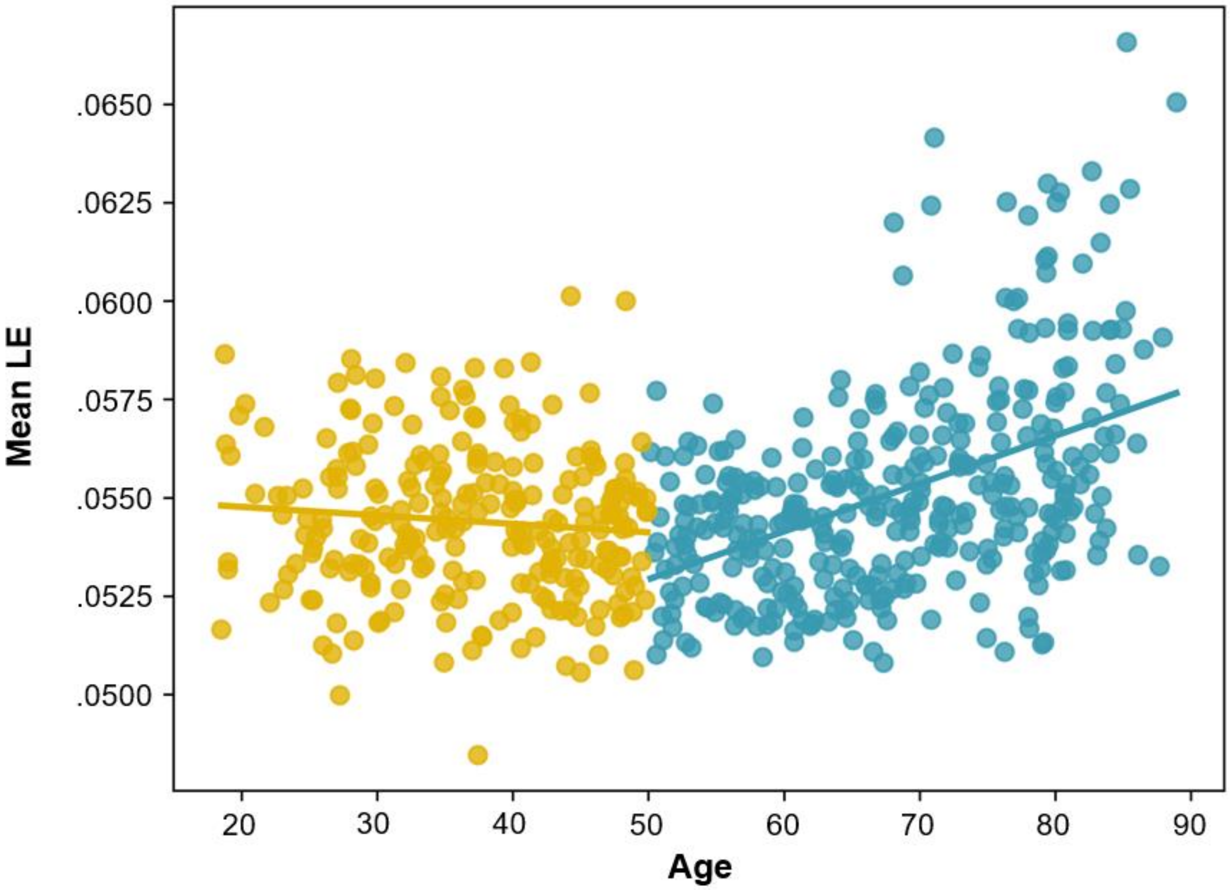

Figure 9. Relationship between age and mean local efficiency (in the regions identified as negatively associated with cognition in OA) for YA (in yellow; $R(242) = -.094$, $p = .143$) and OA (in blue; $R(348) = .461$, $p < .001$).

In order to understand what changes are occurring in the structural connectivity network at the whole-brain level as local efficiency increases in OA, multiple linear regression models were created with mean local efficiency (in the regions identified as negatively associated with cognition in OA) as the dependent variable, and graph theory measures of mean clustering coefficient, mean shortest path length, SC total (total number of SC streamlines in the brain), and mean SC streamline distance as the independent variables. The clustering coefficient and shortest path length were examined as these are measures used to determine whether a network is a small-world network (high clustering coefficient and low shortest path length) as opposed to a random network (low shortest path length but low clustering coefficient). There are many examples of real-world networks that have these small-world properties, including brain networks (Hilgetag et al., 2000; Micheloyannis, Pachou, Stam, Breakspear, et al., 2006; Micheloyannis, Pachou, Stam, Vourkas, et al., 2006; Salvador et al., 2005; Stam et al., 2007). The clustering coefficient measures how likely two neighbors of a region are to also be connected to one another, and supports the ability for subnetworks of the brain to integrate information and be specialized (calculated as a weighted clustering coefficient in this case; Onnela et al., 2005). On the other hand, a low shortest path length (Dijkstra, 1959) indicates that there are short routes between regions in the brain in general, which allows the specialized subnetworks to communicate across the whole brain efficiently (Fornito et al., 2016). Research has identified multiple ways in which small-worldness supports organized functional activity, by improving the capacity for functional segregation as well as integration (Sporns et al., 2000; Sporns & Zwi, 2004), synchronization and propagation of information (Barahona & Pecora, 2002; Hong et al., 2002), computational power (Lago-Fernández et al., 2000), and more (see reviews by Bassett & Bullmore, 2006; Fornito et al., 2016).

Model 1.

Model 1 included independent variables of age, mean clustering coefficient, mean shortest path length, and SC total, with the dependent variable (which will be the same for all models) of local efficiency mean for regions negatively associated with cognition in OA based on the PLS analysis (see Figure 7). For YA, local efficiency decreased with age, was associated with increased clustering coefficient and decreased shortest path length, but was not associated with SC total (see Table 1). For OA, local efficiency *increased* with age, was associated with increased clustering coefficient and decreased shortest path length, and was associated with decreased SC total (see Table 2). These results identified commonalities as well as differences between these age groups in the way that local efficiency impacts the brain network. In both YA and OA increased local efficiency was associated with increased clustering coefficient and decreased shortest path length, indicative of increased small-worldness. However, there were notable differences in Model 1 between YA and OA. Local efficiency was associated with a much larger increase in clustering coefficient in OA (estimate value of 1.442 compared to .713 for YA, which was significant based on the 95% confidence intervals; CI; see Tables 1 and 2), indicating that small-worldness increased more for OA than YA as local efficiency increased. Local efficiency decreased with age in YA, but then increased in OA, and this difference was significant based on the 95% CI. Furthermore, while local efficiency was not associated with SC total for YA, SC total decreased as local efficiency increased in OA, and this group difference was again significant based on the 95% CI. Finally, a much larger amount of variance was accounted for by the model in OA ($R^2 = .635$ compared to $R^2 = .369$ for YA), indicating that local efficiency was associated with more variance in these whole-brain measures.

Table 1. Local Efficiency Multilinear Regression Analysis Model 1 for YA, with dependent variable local efficiency mean for regions negatively associated with cognition in OA based on the PLS analysis. Independent variables included age, mean clustering coefficient, mean shortest path length, and SC total (total SC streamline counts). Model $R^2 = .369$.

Effects	Estimate [95% CI]	Std. Error	*t*-value	*p*-value
Intercept	.079 [.066, .093]	.007	11.499	<.001
Age	$-.566*10^{-4}$ $[-.812*10^{-4}, -.320*10^{-4}]$	$.125*10^{-4}$	-4.540	<.001
Clustering Coefficient	.713 [.473, .953]	.122	5.863	<.001
Shortest Path Length	$-.685*10^{-3}$ $[-.864*10^{-3}, .506*10^{-3}]$	$.907*10^{-4}$	-7.547	<.001
SC Total	$-.200*10^{-4}$ $[-.610*10^{-4}, .210*10^{-4}]$	$.208*10^{-4}$	-.962	.337

Table 2. Local Efficiency Multilinear Regression Analysis Model 1 for OA, with dependent variable local efficiency mean for regions negatively associated with cognition based on the PLS analysis. Independent variables included age, shortest path length, clustering coefficient, and SC total (total SC streamline counts). Model R^2 = .635.

Effects	Estimate [95% CI]	Std. Error	*t*-value	*p*-value
Intercept	.082 [.070, .093]	.006	13.915	<.001
Age	.683*10^{-4} [.503*10^{-4}, .864*10^{-4}]	.919*10^{-5}	7.439	<.001
Clustering Coefficient	1.442 [1.249, 1.635]	.098	14.676	<.001
Shortest Path Length	-.861*10^{-3} [-.103*10^{-2}, -.687*10^{-3}]	.883*10^{-4}	-9.743	<.001
SC Total	-.534*10^{-4} [-.849*10^{-4}, -.220*10^{-4}]	.160*10^{-4}	-3.339	.001

Model 2.

Model 2 included independent variables of age, mean clustering coefficient, mean shortest path length, and mean SC distance. The results for age, clustering coefficient, and shortest path length mirrored those found in Model 1, but additionally we found that SC distance decreased as local efficiency increased for both YA (see Table 3) and OA (see Table 4).

Table 3. Local Efficiency Multilinear Regression Analysis Model 2 for YA, with dependent variable local efficiency mean for regions negatively associated with cognition based on the PLS analysis. Independent variables included age, shortest path length, clustering coefficient, and SC distance (mean of all SC streamline distances). Model R^2 = .399.

Effects	Estimate [95% CI]	Std. Error	*t*-value	*p*-value
Intercept	.082 [.075, .090]	.004	21.858	<.001
Age	-.556*10^{-4} [-.795*10^{-4}, -.317*10^{-4}]	.121*10^{-4}	-4.581	<.001
Clustering Coefficient	.524 [.302, .745]	.112	4.661	<.001
Shortest Path Length	-.673*10^{-3} [-.825*10^{-3}, -.521*10^{-3}]	.774*10^{-4}	-8.696	<.001
SC Distance	-.107*10^{-3} [-.166*10^{-3}, -.485*10^{-4}]	.298*10^{-4}	-3.600	<.001

Table 4. Local Efficiency Multilinear Regression Analysis Model 2 for OA, with dependent variable local efficiency mean for regions negatively associated with cognition based on the PLS analysis. Independent variables included age, shortest path length, clustering coefficient, and SC distance (mean of all SC streamline distances). Model $R^2 = .661$.

Effects	Estimate [95%CI]	Std. Error	*t*-value	*p*-value
Intercept	.074 [.068, .081]	.003	23.129	<.001
Age	$.657*10^{-4}$ [$.482*10^{-4}$, $.831*10^{-4}$]	$.887*10^{-5}$	7.403	<.001
Clustering Coefficient	1.093 [.892, 1.294]	.102	10.704	<.001
Shortest Path Length	$-.679*10^{-3}$ [$-.831*10^{-3}$, $-.528*10^{-3}$]	$.771*10^{-4}$	-8.810	<.001
SC Distance	$-.145*10^{-3}$ [$-.192*10^{-3}$, $-.988*10^{-4}$]	$.237*10^{-4}$	-6.140	<.001

Model 3.

Model 3 included independent variables of age, mean clustering coefficient, mean shortest path length, SC total, and mean SC distance. The results mirrored those found in Models 1 and 2, whereby SC total was not associated with local efficiency for YA but decreased with increasing local efficiency for OA (this group difference was significant based on the 95% CI of the estimate), and SC distance decreased with increasing local efficiency for both YA and OA (see Tables 5 and 6).

Table 5. Local Efficiency Multilinear Regression Analysis Model 3 for YA, with dependent variable local efficiency mean for regions negatively associated with cognition based on the PLS analysis. Independent variables included age, shortest path length, clustering coefficient, SC total (total SC streamline counts), and SC distance (mean of all SC streamline distances). Model $R^2 = .400$.

Effects	Estimate [95% CI]	Std. Error	*t*-value	*p*-value
Intercept	.084 [.070, .097]	.007	12.192	<.001
Age	$-.558*10^{-4}$ [$-.798*10^{-4}$, $-.318*10^{-4}$]	$.122*10^{-4}$	-4.577	<.001
Clustering Coefficient	.539 [.284, .793]	.129	4.173	<.001
Shortest Path Length	$-.683*10^{-3}$ [$-.858*10^{-3}$, $-.508*10^{-3}$]	$.887*10^{-4}$	-7.701	<.001
SC Total	$-.497*10^{-5}$ [$-.460*10^{-4}$, $.360*10^{-4}$]	$.208*10^{-4}$	-.239	.811
SC Distance	$-.106*10^{-3}$ [$-.166*10^{-3}$, $-.456*10^{-4}$]	$.305*10^{-4}$	-3.463	.001

Table 6. Local Efficiency Multilinear Regression Analysis Model 3 for OA, with dependent variable local efficiency mean for regions negatively associated with cognition based on the PLS analysis. Independent variables included age, shortest path length, clustering coefficient, SC total (total SC streamline counts), and SC distance (mean of all SC streamline distances). Model R^2 = .667.

Effects	Estimate [95% CI]	Std. Error	*t*-value	*p*-value
Intercept	.087 [.076, .098]	.006	15.285	<.001
Age	$.639*10^{-4}$ [$.466*10^{-4}$, $.813*10^{-4}$]	$.882*10^{-5}$	7.249	<.001
Clustering Coefficient	1.169 [.962, 1.376]	.105	11.108	<.001
Shortest Path Length	$-.781*10^{-3}$ [$-.949*10^{-3}$, $-.613*10^{-3}$]	$.856*10^{-4}$	-9.126	<.001
SC Total	$-.408*10^{-4}$ [$-.712*10^{-4}$, $-.104*10^{-4}$]	$.155*10^{-4}$	-2.643	.009
SC Distance	$-.136*10^{-3}$ [$-.183*10^{-3}$, $-.899*10^{-4}$]	$.237*10^{-4}$	-5.758	<.001

Taken together with the local efficiency PLS analyses, these results suggest that local efficiency is associated with worse cognition in OA (as shown by the PLS analysis, see Figure 6), and is also associated with less connectivity overall in the brain (SC total) and shorter structural connections (see Table 6). However, local efficiency in these regions increases the small-worldness of the brain network, especially for OA, which has been shown to help support organized network function. This suggests that local efficiency may help shore up the structural brain network in response to other factors in the brain that produce declining cognitive function and decreased structural connections, and this may be accomplished by short-range connections that support local brain function (in line with Heisz et al., 2015).

Discussion

We have demonstrated that changes in the whole-brain SC network are related to cognitive changes with age. However, this relationship is nuanced. There are many structural connections throughout the brain that lose streamlines with age and are associated with declining cognitive abilities, which is expected given the cortical atrophy and demyelination that is known to occur with age. We have also produced the novel demonstration that there are several connections (especially intrahemispheric) that are stronger with age and support spared cognitive function. That these connections are overwhelmingly intrahemispheric supports past research showing that an increase in functional complexity locally and a decrease in complexity involving long-range interactions (especially interhemispheric) occurs in OA, and that this change may be positive as it was associated with better cognitive ability (Heisz et al., 2015). Furthermore, we also identified structural connectivity decreases associated with spared cognition, suggesting that some of the beneficial reorganization of the network involves selective pruning of certain connections.

By applying graph theory to these networks, we investigated these connectivity changes more comprehensively, using nodal efficiency and local efficiency measures. Nodal efficiency measures how well a region is able to communicate with the rest of the brain and is a marker of hubness. We found that non-typical nodal efficiency is detrimental in many brain regions with typically high nodal efficiency, suggesting that there is a relatively ideal network configuration and that alterations are associated with worse cognition. This seems to be the case primarily for regions including the insula, ventrolateral and dorsolateral prefrontal cortex, medial parietal regions, putamen, cingulate cortex, and caudate nucleus. This suggests that more connectivity is not always better, as this can disrupt the ability for the network as a whole to function effectively. However, especially in OA there are a number of regions, particularly in the RH ventral occipital-temporal stream, RH hippocampus, and bilateral nucleus accumbens that relate to better cognition when hubness is increased as measured by nodal efficiency. The nucleus accumbens has been noted in research on the aging brain to be somewhat unique, in that although volume reductions have been noted with age, it is spared from neuronal loss, unlike much of the rest of the brain (see Konar-Nié et al., 2023 for a review). It may be that increasing connectivity bilaterally to this relatively protected subcortical region serves to spare the network, especially considering the role the nucleus accumbens plays in decision making, particularly when there is uncertainty, ambiguity, or when distractors are involved (see Floresco, 2015 for a review). Increasing hubness of the hippocampus was also shown to support cognition. Increasing the global connectivity of the hippocampus may help to preserve the medial temporal lobe memory system, and counteract its susceptibility to degradation in aging and Alzheimer's disease (Beason-Held et al., 2021). The ventral occipital-temporal stream contains a number of modular regions in the fusiform gyrus that are specialized to some extent for specific visual recognition tasks, such as object recognition (lateral occipital complex; Grill-Spector et al., 2001), face recognition (fusiform face area; Kanwisher & Yovel, 2006), visual word recognition (ventral occipitotemporal cortex; Price, 2012), and place recognition (parahippocampal place area Aminoff et al., 2013). It may be that the increase in hubness and connectivity to the ventral occipital-temporal stream helps to maintain the overall network integration of these regions important for tasks relying on visual processing, which are crucial for success on the fluid intelligence test. Furthermore, the ventral stream is implicated as far as the anterior temporal lobe, which has been identified as a crucial hub in the semantic memory network that integrates the multiple modalities involved in semantic memory (Patterson et al., 2007). Semantic memory is unique in that it is one of the few cognitive domains that is spared in general as people age, and is supported by functional changes with age (Hoffman & Morcom, 2018). The increased hubness of the anterior temporal lobe with age may be a structural connectivity factor contributing to robust semantic memory in older adults.

Local efficiency, an indicator of fault tolerance that measures how well connected a region’s neighbors would be if it was removed from the network, was found to be positively associated with cognitive ability in YA for many regions in the brain including cortical regions such as extrastriate cortex, precuneus, retrosplenial cortex, parrahippocampal cortex, medial parietal cortex, temporal and temporoparietal cortex, insula, auditory cortex, and precentral and postcentral gyri, as well as the hippocampus and thalamus in the subcortex. However, the pattern is completely reversed for OA, in which the majority of regions in the brain show a negative association between local efficiency and cognitive ability. By investigating the effect that local efficiency differences have on the whole-brain connectivity patterns, we found that the local efficiency of these regions is associated with greater small-worldness of the brain network throughout the lifespan, but especially so in OA. In OA these local efficiency increases may be in response to declining cognitive ability, declining overall structural connection density, and may use short-range connections to achieve this reorganization.

Limitations and Future Directions

It is important to note that this work is based on the cross-sectional data available to us, rather than the more ideal use of longitudinal data when available. Indeed, recent research has highlighted that there are important differences in what is being measured with cross-sectional and longitudinal data (Vidal-Pineiro et al., 2021). However, we have benefitted greatly from the quality of the Cam-CAN dataset and the ability to observe the lifespan changes in how SC relates to age and cognition over such a large range of ages, from very early adulthood (age 18) to late in the aging process (age 88). Future research with longitudinal data covering a similar age range should investigate these effects from a longitudinal perspective. Furthermore, an investigation of how the SC network grows to support cognition in children and adolescents would contribute to a fuller understanding of how the plastic SC network evolves throughout the entire lifespan.

Conclusion

Whether changes in the functional strategies used by the brain are driving the structural connectivity changes we observed because of the increased use of certain structural connections, or whether the reverse is true, whereby structural connectivity changes are produced in order to encourage new functional strategies, we have demonstrated that healthy aging is not simply a matter of functional adaptations to structural deficiencies. Our findings suggest that not all structural changes are detrimental with age, but rather that functional *and* structural changes occur to spare cognition in older adults. Rather than needing to keep the brain youth-like to maintain cognitive ability, there are multiple ways in which the healthy aging brain represents a unique structural network regime that is distinct from what is ideal for younger adults.

References

Aminoff, E. M., Kveraga, K., & Bar, M. (2013). The role of the parahippocampal cortex in cognition. *Trends in Cognitive Sciences*, *17*(8), 379–390. https://doi.org/10.1016/j.tics.2013.06.009

Barahona, M., & Pecora, L. M. (2002). Synchronization in Small-World Systems. *Physical Review Letters*, *89*(5), 054101. https://doi.org/10.1103/PhysRevLett.89.054101

Bartzokis, G. (2004). Age-related myelin breakdown: A developmental model of cognitive decline and Alzheimer's disease. *Neurobiology of Aging*, *25*(1), 5–18; author reply 49-62. https://doi.org/10.1016/j.neurobiolaging.2003.03.001

Bassett, D. S., & Bullmore, E. (2006). Small-World Brain Networks. *The Neuroscientist*, *12*(6), 512–523. https://doi.org/10.1177/1073858406293182

Beard, J. R., Officer, A., Carvalho, I. A. de, Sadana, R., Pot, A. M., Michel, J.-P., Lloyd-Sherlock, P., Epping-Jordan, J. E., Peeters, G. M. E. E., Mahanani, W. R., Thiyagarajan, J. A., & Chatterji, S. (2016). The World report on ageing and health: A policy framework for healthy ageing. *The Lancet*, *387*(10033), 2145–2154. https://doi.org/10.1016/S0140-6736(15)00516-4

Beason-Held, L. L., Shafer, A. T., Goh, J. O., Landman, B. A., Davatzikos, C., Viscomi, B., Ash, J., Kitner-Triolo, M., Ferrucci, L., & Resnick, S. M. (2021). Hippocampal activation and connectivity in the aging brain. *Brain Imaging and Behavior*, *15*(2), 711–726. https://doi.org/10.1007/s11682-020-00279-6

Cabeza, R., Anderson, N. D., Locantore, J. K., & McIntosh, A. R. (2002). Aging gracefully: Compensatory brain activity in high-performing older adults. *NeuroImage*, *17*(3), 1394–1402. https://doi.org/10.1006/nimg.2002.1280

Cattell, R. B., & Cattell, H. E. P. (1973). *Measuring intelligence with the culture fair tests*. The Institute for Personality and Ability Testing.

Coelho, A., Fernandes, H. M., Magalhães, R., Moreira, P. S., Marques, P., Soares, J. M., Amorim, L., Portugal-Nunes, C., Castanho, T., Santos, N. C., & Sousa, N. (2021). Reorganization of brain structural networks in aging: A longitudinal study. *Journal of Neuroscience Research*, *99*(5), 1354–1376. https://doi.org/10.1002/jnr.24795

Damoiseaux, J. S. (2017). Effects of aging on functional and structural brain connectivity. *NeuroImage*, *160*, 32–40. https://doi.org/10.1016/j.neuroimage.2017.01.077

Davis, S. W., Dennis, N. A., Daselaar, S. M., Fleck, M. S., & Cabeza, R. (2008). Que PASA? The posterior-anterior shift in aging. *Cerebral Cortex (New York, N.Y.: 1991)*, *18*(5), 1201–1209. https://doi.org/10.1093/cercor/bhm155

Dijkstra, E. W. (1959). A note on two problems in connexion with graphs. *Numerische Mathematik*, *1*(1), 269–271.

Efron, B. (1987). Better Bootstrap Confidence Intervals. *Journal of the American Statistical Association*, *82*(397), 171–185. https://doi.org/10.1080/01621459.1987.10478410

Ekstrand, C., Neudorf, J., Kress, S., & Borowsky, R. (2020). Structural connectivity predicts functional activation during lexical and sublexical reading. *NeuroImage*, *218*, 117008. https://doi.org/10.1016/j.neuroimage.2020.117008

Floresco, S. B. (2015). The Nucleus Accumbens: An Interface Between Cognition, Emotion, and Action. *Annual Review of Psychology*, *66*(1), 25–52. https://doi.org/10.1146/annurev-psych-010213-115159

Fornito, A., Zalesky, A., & Bullmore, E. T. (2016). *Fundamentals of brain network analysis*. Elsevier/Academic Press.

Frazier-Logue, N., Wang, J., Wang, Z., Sodums, D., Khosla, A., Samson, A. D., McIntosh, A. R., & Shen, K. (2022). A Robust Modular Automated Neuroimaging Pipeline for Model Inputs to TheVirtualBrain. *Frontiers in Neuroinformatics*, *16*, 883223. https://doi.org/10.3389/fninf.2022.883223

Goñi, J., van den Heuvel, M. P., Avena-Koenigsberger, A., Velez de Mendizabal, N., Betzel, R. F., Griffa, A., Hagmann, P., Corominas-Murtra, B., Thiran, J.-P., & Sporns, O. (2014). Resting-brain functional connectivity predicted by analytic measures of network communication. *Proceedings of the National Academy of Sciences of the United States of America*, *111*(2), Article 2. https://doi.org/10.1073/pnas.1315529111

Grill-Spector, K., Kourtzi, Z., & Kanwisher, N. (2001). The lateral occipital complex and its role in object recognition. *Vision Research*, *41*(10–11), Article 10–11. https://doi.org/10.1016/S0042-6989(01)00073-6

Gu, S., Pasqualetti, F., Cieslak, M., Telesford, Q. K., Yu, A. B., Kahn, A. E., Medaglia, J. D., Vettel, J. M., Miller, M. B., Grafton, S. T., & Bassett, D. S. (2015). Controllability of structural brain networks. *Nature Communications*, *6*(1), Article 1. https://doi.org/10.1038/ncomms9414

Hagmann, P., Cammoun, L., Gigandet, X., Meuli, R., Honey, C. J., Wedeen, V. J., & Sporns, O. (2008). Mapping the Structural Core of Human Cerebral Cortex. *PLOS Biology*, *6*(7), e159. https://doi.org/10.1371/journal.pbio.0060159

Heisz, J. J., Gould, M., & McIntosh, A. R. (2015). Age-related Shift in Neural Complexity Related to Task Performance and Physical Activity. *Journal of Cognitive Neuroscience*, *27*(3), 605–613. https://doi.org/10.1162/jocn_a_00725

Hernandez-Fernandez, M., Reguly, I., Jbabdi, S., Giles, M., Smith, S., & Sotiropoulos, S. N. (2019). Using GPUs to accelerate computational diffusion MRI: From microstructure estimation to tractography and connectomes. *NeuroImage*, *188*, 598–615. https://doi.org/10.1016/j.neuroimage.2018.12.015

Hilgetag, C., Burns, G. A. P. C., O'Neill, M. A., Scannell, J. W., & Young, M. P. (2000). Anatomical connectivity defines the organization of clusters of cortical areas in the macaque and the cat. *Philosophical Transactions of the Royal Society of London. Series B: Biological Sciences*, *355*(1393), 91–110. https://doi.org/10.1098/rstb.2000.0551

Hoffman, P., & Morcom, A. M. (2018). Age-related changes in the neural networks supporting semantic cognition: A meta-analysis of 47 functional neuroimaging studies. *Neuroscience & Biobehavioral Reviews*, *84*, 134–150. https://doi.org/10.1016/j.neubiorev.2017.11.010

Honey, C. J., Thivierge, J.-P., & Sporns, O. (2010). Can structure predict function in the human brain? *NeuroImage*, *52*(3), Article 3. https://doi.org/10.1016/j.neuroimage.2010.01.071

Hong, H., Choi, M. Y., & Kim, B. J. (2002). Synchronization on small-world networks. *Physical Review. E, Statistical, Nonlinear, and Soft Matter Physics*, *65*(2 Pt 2), 026139. https://doi.org/10.1103/PhysRevE.65.026139

Ilalan, D., & Pirgaip, B. (2019). The Impact of US Dollar Index on Emerging Stock Markets: A Simultaneous Granger Causality and Rolling Correlation Analysis. In R. Biswas & M. Michaelides (Eds.), *Essays in Financial Economics* (Vol. 35, pp. 145–154). Emerald Publishing Limited. https://doi.org/10.1108/S0196-382120190000035007

Jenkinson, M., Beckmann, C. F., Behrens, T. E. J., Woolrich, M. W., & Smith, S. M. (2012). FSL. *NeuroImage*, *62*(2), Article 2. https://doi.org/10.1016/j.neuroimage.2011.09.015

Kanwisher, N., & Yovel, G. (2006). The fusiform face area: A cortical region specialized for the perception of faces. *Philosophical Transactions of the Royal Society B: Biological Sciences*, *361*(1476), 2109–2128. https://doi.org/10.1098/rstb.2006.1934

Konar-Nié, M., Guzman-Castillo, A., Armijo-Weingart, L., & Aguayo, L. G. (2023). Aging in nucleus accumbens and its impact on alcohol use disorders. *Alcohol*, *107*, 73–90. https://doi.org/10.1016/j.alcohol.2022.08.004

Kovacevic, N., Abdi, H., Beaton, D., & McIntosh, A. R. (2013). Revisiting PLS Resampling: Comparing Significance Versus Reliability Across Range of Simulations. In H. Abdi, W. W. Chin, V. Esposito Vinzi, G. Russolillo, & L. Trinchera (Eds.), *New Perspectives in Partial Least Squares and Related Methods* (pp. 159–170). Springer. https://doi.org/10.1007/978-1-4614-8283-3_10

Lago-Fernández, L. F., Huerta, R., Corbacho, F., & Sigüenza, J. A. (2000). Fast Response and Temporal Coherent Oscillations in Small-World Networks. *Physical Review Letters*, *84*(12), 2758–2761. https://doi.org/10.1103/PhysRevLett.84.2758

Madden, D. J., Jain, S., Monge, Z. A., Cook, A. D., Lee, A., Huang, H., Howard, C. M., & Cohen, J. R. (2020). Influence of Structural and Functional Brain Connectivity on Age-Related Differences in Fluid Cognition. *Neurobiology of Aging*, *96*, 205–222. https://doi.org/10.1016/j.neurobiolaging.2020.09.010

McIntosh, A. R., & Lobaugh, N. J. (2004). Partial least squares analysis of neuroimaging data: Applications and advances. *NeuroImage*, *23 Suppl 1*, S250-263. https://doi.org/10.1016/j.neuroimage.2004.07.020

Micheloyannis, S., Pachou, E., Stam, C. J., Breakspear, M., Bitsios, P., Vourkas, M., Erimaki, S., & Zervakis, M. (2006). Small-world networks and disturbed functional connectivity in schizophrenia. *Schizophrenia Research*, *87*(1), 60–66. https://doi.org/10.1016/j.schres.2006.06.028

Micheloyannis, S., Pachou, E., Stam, C. J., Vourkas, M., Erimaki, S., & Tsirka, V. (2006). Using graph theoretical analysis of multi channel EEG to evaluate the neural efficiency hypothesis. *Neuroscience Letters*, *402*(3), 273–277. https://doi.org/10.1016/j.neulet.2006.04.006

Nelson, N. A., Jacobucci, R., Grimm, K. J., & Zelinski, E. M. (2020). The bidirectional relationship between physical health and memory. *Psychology and Aging*, *35*(8), 1140–1153. https://doi.org/10.1037/pag0000579

Neudorf, J., Ekstrand, C., Kress, S., & Borowsky, R. (2020). Brain structural connectivity predicts brain functional complexity: Diffusion tensor imaging derived centrality accounts for variance in fractal properties of functional magnetic resonance imaging signal. *Neuroscience*, *438*, 1–8. https://doi.org/10.1016/j.neuroscience.2020.04.048

Neudorf, J., Kress, S., & Borowsky, R. (2022). Structure can predict function in the human brain: A graph neural network deep learning model of functional connectivity and centrality based on structural connectivity. *Brain Structure and Function*, *227*(1), 331–343. https://doi.org/10.1007/s00429-021-02403-8

Onnela, J.-P., Saramäki, J., Kertész, J., & Kaski, K. (2005). Intensity and coherence of motifs in weighted complex networks. *Physical Review E*, *71*(6), 065103. https://doi.org/10.1103/PhysRevE.71.065103

Patterson, K., Nestor, P. J., & Rogers, T. T. (2007). Where do you know what you know? The representation of semantic knowledge in the human brain. *Nature Reviews Neuroscience*, *8*(12), 976–987. https://doi.org/10.1038/nrn2277

Price, C. J. (2012). A review and synthesis of the first 20years of PET and fMRI studies of heard speech, spoken language and reading. *NeuroImage*, *62*(2), Article 2. https://doi.org/10.1016/j.neuroimage.2012.04.062

Pur, D. R., Preti, M. G., de Ribaupierre, A., Van De Ville, D., Eagleson, R., Mella, N., & de Ribaupierre, S. (2022). Mapping of Structure-Function Age-Related Connectivity Changes on Cognition Using Multimodal MRI. *Frontiers in Aging Neuroscience*, *14*. https://www.frontiersin.org/articles/10.3389/fnagi.2022.757861

Rosenthal, G., Váša, F., Griffa, A., Hagmann, P., Amico, E., Goñi, J., Avidan, G., & Sporns, O. (2018). Mapping higher-order relations between brain structure and function with embedded vector representations of connectomes. *Nature Communications*, *9*(1), Article 1. https://doi.org/10.1038/s41467-018-04614-w

Salat, D. H., Buckner, R. L., Snyder, A. Z., Greve, D. N., Desikan, R. S. R., Busa, E., Morris, J. C., Dale, A. M., & Fischl, B. (2004). Thinning of the Cerebral Cortex in Aging. *Cerebral Cortex*, *14*(7), 721–730. https://doi.org/10.1093/cercor/bhh032

Salvador, R., Suckling, J., Coleman, M. R., Pickard, J. D., Menon, D., & Bullmore, E. (2005). Neurophysiological Architecture of Functional Magnetic Resonance Images of Human Brain. *Cerebral Cortex*, *15*(9), 1332–1342. https://doi.org/10.1093/cercor/bhi016

Sarwar, T., Tian, Y., Yeo, B. T. T., Ramamohanarao, K., & Zalesky, A. (2021). Structure-function coupling in the human connectome: A machine learning approach. *NeuroImage*, *226*, 117609. https://doi.org/10.1016/j.neuroimage.2020.117609

Schaefer, A., Kong, R., Gordon, E. M., Laumann, T. O., Zuo, X.-N., Holmes, A. J., Eickhoff, S. B., & Yeo, B. T. T. (2018). Local-Global Parcellation of the Human Cerebral Cortex from

Intrinsic Functional Connectivity MRI. *Cerebral Cortex*, *28*(9), 3095–3114. https://doi.org/10.1093/cercor/bhx179

Schirner, M., McIntosh, A. R., Jirsa, V., Deco, G., & Ritter, P. (2018). Inferring multi-scale neural mechanisms with brain network modelling. *eLife*, *7*, e28927. https://doi.org/10.7554/eLife.28927

Shafto, M. A., Tyler, L. K., Dixon, M., Taylor, J. R., Rowe, J. B., Cusack, R., Calder, A. J., Marslen-Wilson, W. D., Duncan, J., Dalgleish, T., Henson, R. N., Brayne, C., Matthews, F. E., & Cam-CAN. (2014). The Cambridge Centre for Ageing and Neuroscience (Cam-CAN) study protocol: A cross-sectional, lifespan, multidisciplinary examination of healthy cognitive ageing. *BMC Neurology*, *14*(1), 204. https://doi.org/10.1186/s12883-014-0204-1

Sporns, O. (2018). Graph theory methods: Applications in brain networks. *Dialogues in Clinical Neuroscience*, *20*(2), 111–121.

Sporns, O., Tononi, G., & Edelman, G. M. (2000). Theoretical neuroanatomy: Relating anatomical and functional connectivity in graphs and cortical connection matrices. *Cerebral Cortex (New York, N.Y.: 1991)*, *10*(2), 127–141. https://doi.org/10.1093/cercor/10.2.127

Sporns, O., & Zwi, J. D. (2004). The small world of the cerebral cortex. *Neuroinformatics*, *2*(2), 145–162. https://doi.org/10.1385/NI:2:2:145

Stam, C., Jones, B., Nolte, G., Breakspear, M., & Scheltens, P. (2007). Small-World Networks and Functional Connectivity in Alzheimer's Disease. *Cerebral Cortex*, *17*(1), 92–99. https://doi.org/10.1093/cercor/bhj127

Tian, Y., Margulies, D. S., Breakspear, M., & Zalesky, A. (2020). Topographic organization of the human subcortex unveiled with functional connectivity gradients. *Nature Neuroscience*, *23*(11), Article 11. https://doi.org/10.1038/s41593-020-00711-6

United Nations. (2022). *UNCITRAL Expedited Arbitration Rules 2021: UNCITRAL Rules on Transparency in Treaty-based Investor-State Arbitration.* United Nations. https://doi.org/10.18356/9789210021753

van den Heuvel, M. P., & Sporns, O. (2011). Rich-Club Organization of the Human Connectome. *Journal of Neuroscience*, *31*(44), 15775–15786. https://doi.org/10.1523/JNEUROSCI.3539-11.2011

van den Heuvel, M. P., & Sporns, O. (2013). Network hubs in the human brain. *Trends in Cognitive Sciences*, *17*(12), 683–696. https://doi.org/10.1016/j.tics.2013.09.012

Vidal-Pineiro, D., Wang, Y., Krogsrud, S. K., Amlien, I. K., Baaré, W. F., Bartres-Faz, D., Bertram, L., Brandmaier, A. M., Drevon, C. A., Düzel, S., Ebmeier, K., Henson, R. N., Junqué, C., Kievit, R. A., Kühn, S., Leonardsen, E., Lindenberger, U., Madsen, K. S., Magnussen, F., … Fjell, A. (2021). Individual variations in 'brain age' relate to early-life factors more than to longitudinal brain change. *eLife*, *10*, e69995. https://doi.org/10.7554/eLife.69995

Supplemental Materials

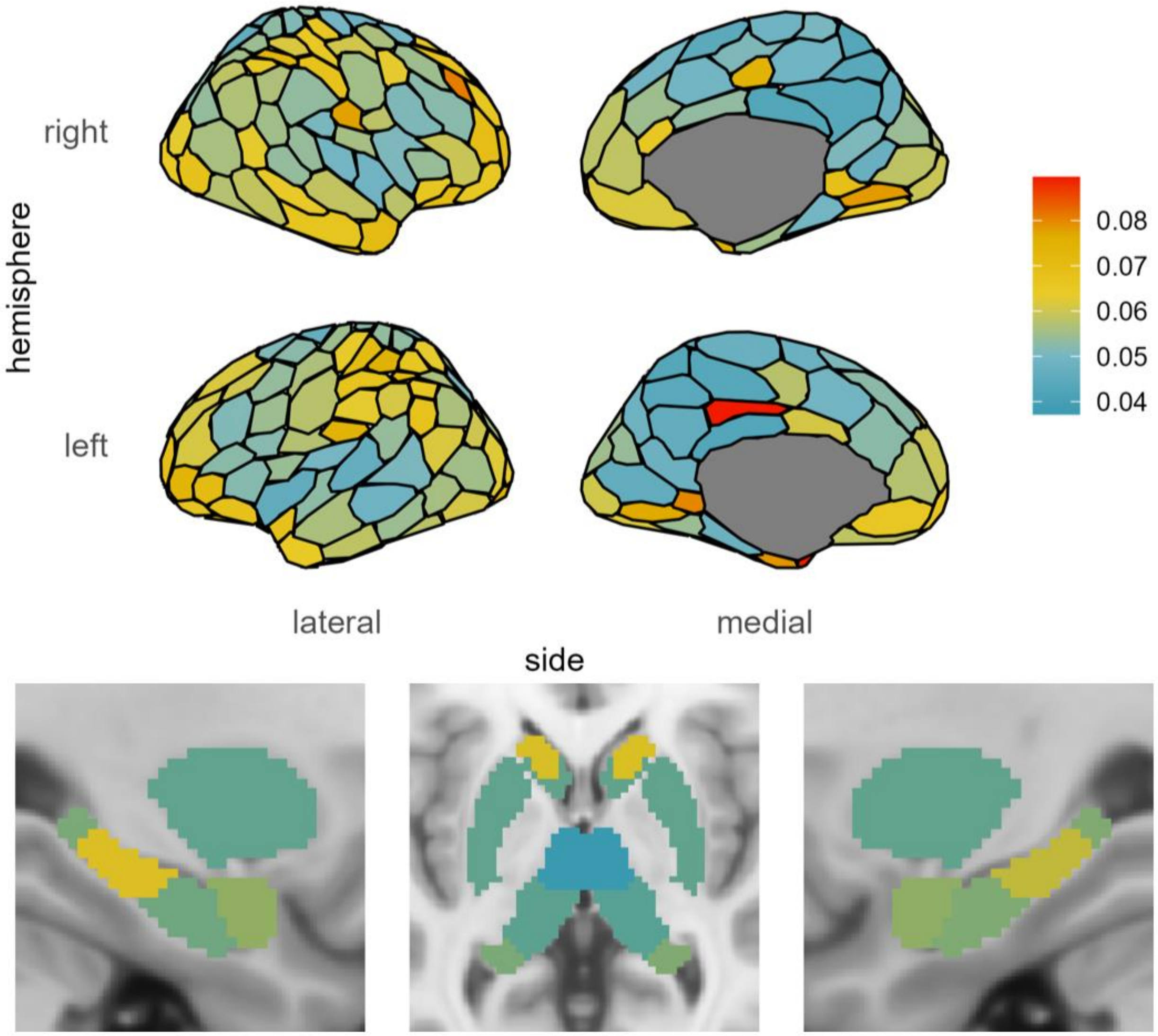

Supplementary Figure 1. Brain map of mean local efficiency for all participants.